Proc. Natl. Acad. Sci. USA
Vol. 92, pp. 1222–1226, February 1995
Biochemistry

The structure of unliganded reverse transcriptase from the human immunodeficiency virus type 1

(x-ray crystallography/polymerase/antiviral drugs)

D. W. RODGERS*, S. J. GAMBLIN*†, B. A. HARRIS*, S. RAY*†, J. S. CULP‡, B. HELLMIG‡, D. J. WOOLF‡, C. DEBOUCK§, AND S. C. HARRISON*†¶

*Department of Molecular and Cellular Biology and †Howard Hughes Medical Institute, Harvard University, Cambridge, MA 02138; and Departments of ‡Protein Biochemistry and §Molecular Genetics, SmithKline Beecham Pharmaceuticals, King of Prussia, PA 19406

Contributed by S. C. Harrison, November 2, 1994

ABSTRACT **The crystal structure of the reverse transcriptase (RT) from the type 1 human immunodeficiency virus has been determined at 3.2-Å resolution. Comparison with complexes between RT and the polymerase inhibitor Nevirapine [Kohlstaedt, L. A., Wang, J., Friedman, J. M., Rice, P. A. & Steitz, T. A. (1992) *Science* 256, 1783–1790] and between RT and an oligonucleotide [Jacobo-Molina, A., Ding, J., Nanni, R., Clark, A. D., Lu, X., Tantillo, C., Williams, R. L., Kamer, G., Ferris, A. L., Clark, P., Hizi, A., Hughes, S. H. & Arnold, E. (1993) *Proc. Natl. Acad. Sci. USA* 90, 6320–6324] reveals changes associated with ligand binding. The enzyme is a heterodimer (p66/p51), with domains labeled "fingers," "thumb," "palm," and "connection" in both subunits, and a ribonuclease H domain in the larger subunit only. The most striking difference between RT and both complex structures is the change in orientation of the p66 thumb (≈33° rotation). Smaller shifts relative to the core of the molecule were also found in other domains, including the p66 fingers and palm, which contain the polymerase active site. Within the polymerase catalytic region itself, there are no rearrangements between RT and the RT/DNA complex. In RT/Nevirapine, the drug binds in the p66 palm near the polymerase active site, a region that is well-packed hydrophobic core in the unliganded enzyme. Room for the drug is provided by movement of a small β-sheet within the palm domain of the Nevirapine complex. The rearrangement within the palm and thumb, as well as domain shifts relative to the enzyme core, may prevent correct placement of the oligonucleotide substrate when the drug is bound.**

The reverse transcriptase (RT) from the type 1 human immunodeficiency virus type 1 (HIV-1) is a heterodimer composed of a 66-kDa subunit (p66) and a 51-kDa subunit (p51) derived from p66 by proteolytic removal of the C-terminal domain. RT possesses both DNA polymerase activity, which ultimately produces double-stranded DNA from the viral genomic RNA, and a ribonuclease H (RNase H) activity, which cleaves the viral genome after it is copied. A crystal structure of RT complexed with the drug Nevirapine (RT/Nevirapine), a non-nucleoside-analog polymerase inhibitor, has been reported (1, 2), as well as the structure (3) of a complex with an 18/19-mer oligonucleotide (RT/DNA). We report here the structure of the unliganded enzyme at 3.2-Å resolution.‖ By comparing it with RT/Nevirapine and RT/DNA, we can begin to examine the mechanisms of drug and nucleic acid binding. These processes are found to involve changes in domain arrangement within the enzyme but no major repositioning of the polymerase catalytic residues. Differences between the unliganded enzyme and RT/Nevirapine suggest a possible mechanism for the action of nonnucleoside inhibitors.

The publication costs of this article were defrayed in part by page charge payment. This article must therefore be hereby marked "*advertisement*" in accordance with 18 U.S.C. §1734 solely to indicate this fact.

MATERIALS AND METHODS

Crystallization. Expression and purification of HIV-1 (BH10 strain) RT have been described (4, 5). The recombinant RT used in this study was produced by processing of a *pol* precursor by the HIV-1 protease and should be identical to the enzyme produced by the virus. Crystals were grown at 4°C by vapor diffusion in hanging or sitting drops. A 30 mg/ml solution of the enzyme [75 mM sodium phosphate (pH 6.8)/1–2 mM dithiothreitol] was mixed with an equal volume of well solution containing 33–35% ammonium sulfate/100 mM sodium phosphate, pH 6.8. Crystals grew to ≈0.15 × 0.40 × 0.02 mm. Two forms were found: one in space group F222 (a = 162.3 Å, b = 168.6 Å, c = 641.2 Å, $\alpha = \beta = \gamma = 90.0°$), and the other in space group C2 (a = 168.7 Å, b = 162.8 Å, c = 331.8 Å, β = 105.7°) with closely related packing.

Data Collection. RT crystals used for data collection were dialyzed against buffer containing 50% ammonium sulfate, 60 mM sodium phosphate (pH 6.8), and 20% (vol/vol) glycerol. Crystals were mounted in loops (6) made from nylon fibers and flash-cooled in the gaseous nitrogen stream from a modified commercial cryostat. The crystals were then stored in liquid nitrogen, sometimes after preliminary assessment using a rotating anode generator, and transported to the Cornell High Energy Synchrotron Source (CHESS) for data collection on the F1 and A1 lines (λ = 0.91 Å). Data were recorded on Fuji imaging phosphor plates from crystals maintained at −165°C. A low-resolution data set (to 5.5 Å) was collected from a single F222 crystal using 1.5–2.0° oscillations. Higher-resolution data were collected from the C2 crystal form using smaller oscillation angles, most frequently 0.5°. Between 5° and 10° of data could be collected within the effective lifetime of a single crystal, and the final C2 data set contained observations from 34 crystals. The HKL package (Z. Otwinowsky, University of Texas Southwestern Medical School, and W. Minor, Purdue University) was used to reduce, scale, and postrefine the data. The overall R_{merge} of the C2 data set to 3.2 Å was 13.3%, with an average redundancy of 3.3 and 85% of the possible reflections recorded.

Structure Determination and Refinement. A polyalanine model was built, using the program O (7), from the RT/DNA complex Cα atom coordinates (3). This model was used to

Abbreviations: RT, reverse transcriptase; HIV-1, human immunodeficiency virus type 1; RT/Nevirapine, crystal structure of reverse transcriptase complex with Nevirapine; RT/DNA, crystal structure of reverse transcriptase complex with a double-stranded DNA; RNase H, ribonuclease H.

¶To whom reprint requests should be sent at the * address.

‖The atomic coordinates and structure factors have been deposited in the Protein Data Bank, Chemistry Department, Brookhaven National Laboratory, Upton, NY 11973 (Entry 1HMZ).

determine a molecular replacement solution with the AMORE (8) and CCP4 packages (Science and Engineering Research Council Collaborative Computing Project, Daresbury Laboratory). The F222 crystal form contains two RT heterodimers in the asymmetric unit related primarily by a translation operation, and the C2 form contains two of these translationally related pairs. Cross rotation and translation function calculations gave consistent solutions in the two crystal forms, resulting in packing arrangements that differed by only a few Ångstroms as expected. For the C2 data, which were used in subsequent work, averaging transformations were more accurately determined for the 36 domains in the asymmetric unit by real space refinement against omit maps, using RAVE (9). Side chains were then added, and the model was rebuilt into 4-fold averaged omit density. The rebuilt model gave an R_{free} of 0.47 using data to 3.2 Å, but extensive attempts to refine the model with XPLOR (10) produced no significant improvement. A translation function calculation (CCP4) with the rebuilt model indicated a shift of 4 Å along the *a* axis of the unit cell. After applying this translation, refinement lowered the R_{free} to 0.41. Rounds of model building (always against averaged omit maps), including addition of a Mg^{2+} ion to the RNase H active site, and local-symmetry-restrained refinement gave an R_{free} of 0.30 (0.40 at 3.2 Å) and $R_{working}$ of 0.26 (0.38 at 3.2 Å) for the model reported here. Final geometry parameters are within established values (rms bond lengths, 0.01 Å; rms bond angles, 1.8°; rms torsion angles, 20.7°).

RESULTS AND DISCUSSION

Overview of the HIV-1 RT. A representation of the HIV-1 RT heterodimer is shown in Fig. 1. Domains have been named (1), in part, for the resemblance of the p66 domain to a right hand. The p66 subunit consists of fingers (blue), palm (red), thumb (green), connection (yellow), and RNase H (brown) domains. The first four of these domains have counterparts in the smaller p51 subunit. Despite identical sequences and similar internal structure, the four corresponding domains in p66 and p51 are arranged differently (1, 3). In particular, the thumb and connection domains roughly exchange places in the two subunits.

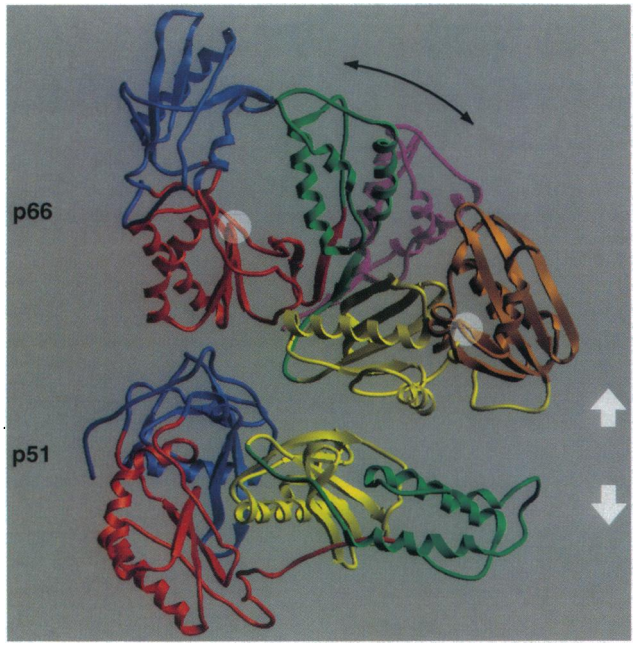

FIG. 1. Domain structure of the HIV-1 reverse transcriptase. The two subunits of the heterodimer have been separated as indicated by the white arrows. Domains are coded by color: blue, fingers (residues 1–84 and 120–150); red, palm (85–119 and 151–243); green, thumb (244–322); yellow, connection (323–437); brown, RNase H (438–556). The thumb domain from the superposed RT/DNA complex (3) is drawn in light purple, with an arrow indicating its different orientation from the thumb of unliganded RT. Polymerase (p66 palm domain) and RNase H active sites are indicated by white disks. All figures were produced with the program RIBBONS (11).

The two catalytic sites, polymerase and RNase H, are indicated in Fig. 1. In the cocrystal structure of RT with duplex DNA (3), one end of the oligonucleotide lies near the polymerase catalytic site of the p66 palm, in a large gap between the fingers and thumb domains, which both make important DNA contacts. There is a similar large opening between the p66 fingers and thumb in the complex with the nonnucleoside inhibitor Nevirapine (1, 2). The most striking feature of the unliganded RT structure presented here is that this large opening no longer exists because the thumb domain assumes a different position. In Fig. 1, the p66 thumb of RT is drawn in green, and the thumb from the RT/DNA complex is in purple. An arrow indicates the shift in orientation of the thumb between the two structures. In contrast to the open conformation of the RT/DNA complex, the RT thumb lies over the polymerase active site of the palm, actually coming into contact with a portion of the fingers domain. With the thumb in this position, the enzyme cannot accommodate its template/primer substrate. This orientation is also incompatible with nonnucleoside inhibitor binding (see below).

Domain Rearrangements in RT Structures. While the p66 thumb domain movement is the most apparent difference between the RT structure and the RT/Nevirapine (1, 2) and RT/DNA (3) complexes, there are also more subtle changes in the relative positions of other domains. Comparison of superpositions between the three structures based on individual domains indicates that there is a conserved core region of the enzyme that varies only within the expected error limits of the structures. This invariant region consists of the p66 connection domain, and the p51 fingers, thumb, and connection domains. Superposition based on this core provides a useful frame for comparing overall differences between the three RT structures. This view is shown in Fig. 2 *Upper* for RT and the RT/Nevirapine complex, and in Fig. 2 *Lower* for RT and the RT/DNA complex.

The invariant core is drawn in light purple for both RT and RT/Nevirapine in Fig. 2 *Upper*. In dark purple are the domains of RT/Nevirapine that deviate substantially from their positions in the unliganded enzyme. As noted above, the change in thumb position is the largest movement, requiring a rotation of 34° for a best fit. The p66 fingers and palm domains also shift, however, moving primarily as a single, rigid unit. Rotation by 9.9° and translation by 2.7 Å is required to superimpose these domains from the two molecules. This moves most parts of the palm domain in RT/Nevirapine slightly toward the gap between the fingers and thumb, while the fingers domain moves away from the thumb, further opening the large cleft in the molecule. In addition to these changes near the polymerase active site, the orientation of the p66 RNase H domain also differs in the two structures.

In the RT/DNA complex (Fig. 2*B*, purple), the rotation of the thumb (32° relative to RT) places it in an orientation similar to the thumb in the RT/Nevirapine complex. The fingers and palm in RT/DNA also move as a rigid unit, but the change from their position in RT is smaller (5.9° rotation; 1.6 Å translation). Here, the altered conformation moves the palm domain away from the gap between the fingers and thumb by up to 3 Å, a shift in the opposite direction to RT/Nevirapine. The fingers domain is close to its position in the unliganded enzyme, again in contrast to the drug complex. Significant changes in the position of the p51 palm domain also occur.

RT is clearly a flexible molecule, and it is possible that some rearrangements result from forces associated with different

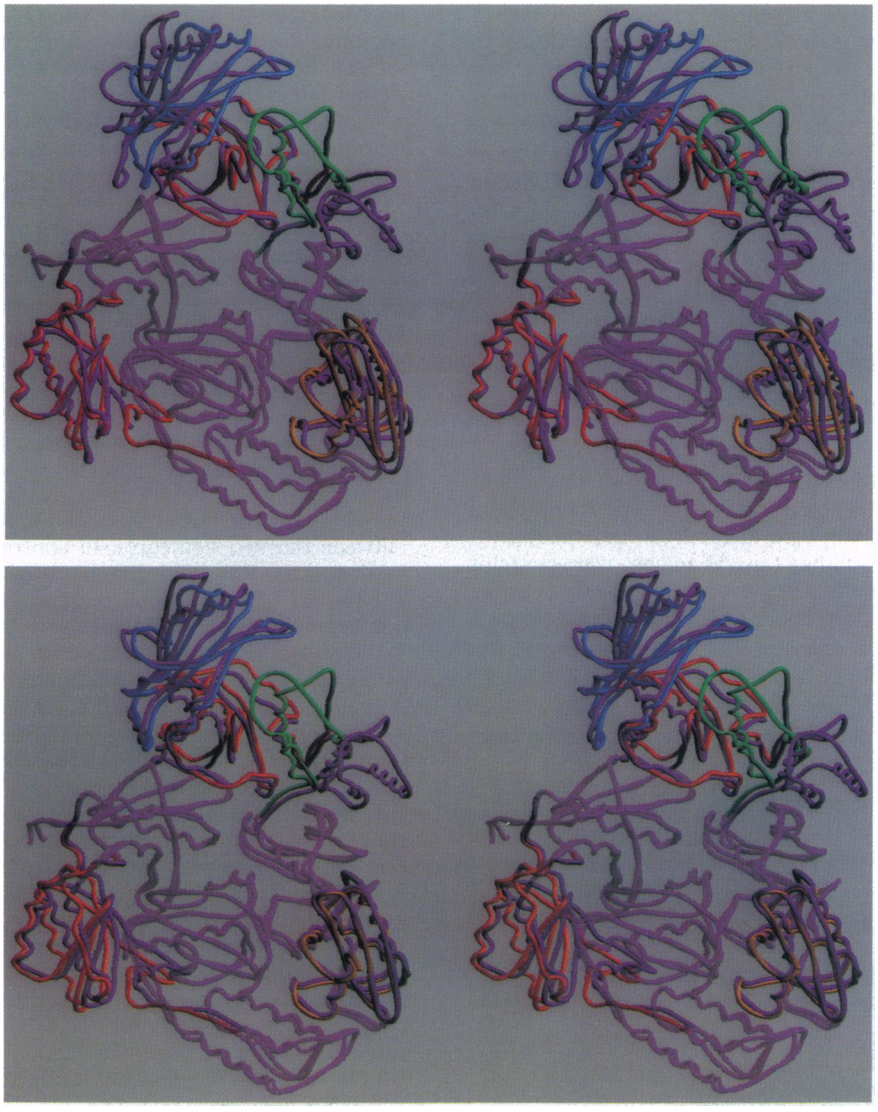

FIG. 2. Superpositions of RT with the RT/Nevirapine (*Upper*) (1, 2) and RT/DNA (*Lower*) (3) complexes shown as stereoviews. Cα traces of the core region (see text) used for superposition are shown in light purple for all molecules. More variable domains are shown in the domain colors for RT (see Fig. 1) and in dark purple for the superposed complexes. In the core region, RT and the complexes superpose with rms values of 2.2 Å (RT/Nevirapine) and 2.1 Å (RT/DNA) on Cα atoms.

crystal environments. However, the four heterodimers in the asymmetric unit of the RT crystals show only small variations in domain arrangement. In this case, the different environments do not greatly influence conformation. Also, another structure of unliganded RT, which conforms closely to the model described here, has been determined** from crystals with different packing. It seems probable that the domain rearrangements in the RT complexes arise from ligand binding.

Description of Palm and Thumb Regions and Comparison with the Nevirapine Complex. Superposing the available RT models based on the structurally invariant core region shows the large relative shifts of the p66 fingers, palm, and thumb domains. A more useful frame for comparing the local geometry of the active site and nonnucleoside inhibitor binding region is superposition based on p66 palm residues alone. This view is shown in Fig. 3 *Upper* for parts of the palm and thumb domains of the unliganded enzyme and superposed Nevirapine complex (1, 2). Three elements are shown: the portion of β-sheet, composed of β6 and the β9–10 hairpin, which contains the catalytic aspartate residues (shown as white spheres); an adjacent small sheet formed from β-strands 12, 13, and 14; and the extreme N- and C-terminal portions of the thumb domain (in green for the unliganded enzyme). Also shown in Fig. 3 *Upper* are many of the side chains from unliganded RT positioned in or near the binding site for the nonnucleoside class of RT inhibitors. Fig. 3 *Upper Inset* shows the same region of RT/Nevirapine with the drug and side chains indicated.

The superposed RT/Nevirapine complex is drawn in purple. In this reference frame, the sheet containing the catalytic aspartate residues (β6, β9, and β10) is nearly identical in the two structures. Although not shown in Fig. 3, this structural agreement extends to the two helices that underlie the sheet and up through the entire fingers domain. Thus the main-chain path in the fingers and major part of the palm domain is not altered by Nevirapine binding. In contrast, the small sheet formed by β-strands 12, 13, and 14 (residues 224–241) shifts in the drug complex as a rigid unit toward the thumb domain, rotating relative to the corresponding element in RT. This rotation of its base displaces the thumb from the closed

**Raag, R., Clark, A. D., Jr., Ding, J., Jocobo-Molina, A., Lu, X., Nanni, R. G., Tantillo, C., Hughes, S. H. & Arnold, E., American Crystallographic Association Meeting, June 25–July 1, 1994, p. B03 (abstr.).

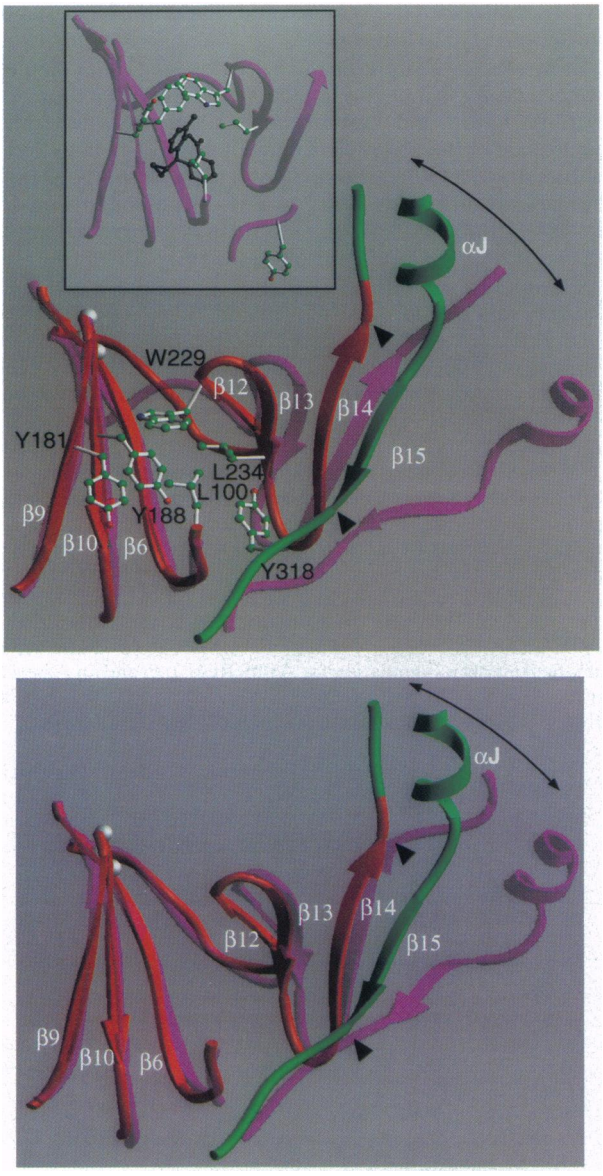

FIG. 3. Portions of the RT p66 palm and thumb domains with superposed RT/Nevirapine (*Upper*) and RT/DNA complexes (*Lower*). Superpositions were based on palm domain Cα atom coordinates. RT is colored in red and green, and the complexes are shown in light purple. Side-chain atoms from some residues near the nonnucleoside inhibitor site are included in *Upper*. *Upper Inset* shows the drug (black) binding site in the RT/Nevirapine complex (1, 2). The key side chains in their altered positions are also shown. Catalytic aspartate residues at the polymerase active site are shown as white spheres. The large arrows show the change in thumb position between the unliganded and complex structures, and the arrowheads indicate hinge points in the thumb (see text).

position, breaking the contact with the fingers and opening up the active-site cleft (see large arrow in Fig. 3 *Upper*).

Repositioning the thumb domain in RT/Nevirapine involves, in addition to the rotation of its base, a hinge-like motion around Pro-243 on the N-terminal end and Val-317 on the C-terminal end (see arrowheads in Fig. 3 *Upper*). This 17° rotation may simply result from forces associated with a packing contact made by the thumb in the RT/Nevirapine crystals. Other differences between the two models occur in the path of the chain N-terminal to the β12–14 sheet, perhaps to accommodate the different 12–14 sheet positions, and in the chain N-terminal to β11 (data not shown), which runs from the fingers domain across β9 to form one side of the nonnucleoside inhibitor binding site.

The structure of unliganded RT suggests a straightforward explanation for the changes in the Nevirapine complex. In RT, the binding site for Nevirapine is not a pocket or cavity, but a region of well-packed hydrophobic core (see Fig. 3 *Upper*), which extends continuously up into the thumb. There are no cavities overlapping the drug-binding site large enough to contain even a single water molecule. Therefore residues must be displaced to accommodate the drug. (In fact, it is unlikely that this site would have been recognized as a target for drug design from the unliganded structure alone.) Nevirapine from the complex overlaps primarily with Tyr-188 and Trp-229 in the unliganded enzyme and, to a lesser degree, with Leu-100, Tyr-181, and Leu-234. Together these residues occupy 74% of the van der Waals volume of the superposed drug. The key event in creating space for the drug is the shift and rotation of the sheet formed by β12–14. This movement withdraws, in particular, Trp-229 from the drug-binding site (see Fig. 3 *Upper Inset*). There is then room for the Tyr-181 and Tyr-188 side chains to assume the rotamer conformations found in the Nevirapine complex (2), pointing toward the catalytic aspartate residues rather than away from them as in RT. Withdrawing Trp-229 and flipping the two tyrosine side chains creates most of the space necessary to accommodate the drug.

Comparison with the RT/DNA Complex. A close-up view of the p66 palm and base of the thumb is shown in Fig. 3 *Lower* for RT (red and green), together with a local superposition of the complex between RT and an 18/19-mer DNA fragment (purple; ref. 3). Like the Nevirapine/RT complex (Fig. 3 *Upper*; see previous section), the sheet composed of β6 and β9–10, which contains the catalytic aspartate residues (white spheres), has the same main-chain path in both models, as do the underlying helices and the fingers domain. Unlike the Nevirapine complex, however, the small sheet formed by β12–14 remains very close to its original position in RT, and there is no shift or rotation at the thumb base. From published reports (3, 12), it appears that the similarity in main-chain position holds for side-chain orientations in the region of the nonnucleoside inhibitor site. In particular, the position of Trp-229 is roughly the same in the RT/DNA complex, as are the rotamer conformations of Tyr-181 and Tyr-188. This similarity suggests that the dependence of some inhibitor compounds on prior template-primer binding (13) is not due to any major rearrangements in the drug-binding site.

The p66 thumb domain in the RT/DNA complex is rotated into an open position (large arrow in Fig. 3 *Lower*), forming one side of a clamp for the DNA fragment. Helices in the thumb make extensive contacts to the sugar-phosphate backbone of the primer and template strands, respectively. The motion of the thumb as it swings out to accommodate the DNA involves only the second of the two components described for its shift in the RT/Nevirapine complex. There is no rotation at the base of the thumb. Instead, there is only a hinge-like motion at the same residues as in the drug complex, Pro-243 and Val-317 (arrowheads). However, the rotation at this point is 29°, much greater than the corresponding 17° rotation in RT/Nevirapine. This larger hinge motion places the thumbs in the RT/DNA and RT/Nevirapine complexes just a few degrees apart. Thus, they achieve equivalent positions in different ways.

The differences in the way the thumbs open up from the closed position in RT suggest a possible mechanism for the action of the nonnucleoside inhibitors. The β12–13 hairpin is an important contact region for the primer strand in the RT/DNA complex (3), and its different position in the two complex structures might affect placement of the template-primer relative to the catalytic residues, modulating activity. Differences in the final positions of the template-primer might also occur as a result of the overall shifts in the p66 fingers, palm, and thumb regions relative to the conserved core (see above), which binds a portion of the DNA fragment. Changes

in the interaction between RT and the template-primer on binding nonnucleoside inhibitors have been suggested based on measurements of activity (14) and on fluorescence (15) studies. Another possibility is that the drug alters the position or orientation of catalytically important residues in the active site. The comparison here shows that the main-chain path is not altered locally by either nucleic acid or drug binding. Small differences are found in side-chain positions of the catalytic aspartates, but the accuracy of current models is insufficient to evaluate the significance of these changes.

Interaction of the Thumb and Fingers Domains. The contact between the fingers and thumb domain in RT (see Fig. 1) is formed by an extended chain region in the fingers (residues 61 and 74–78) and the loop between helices αI and αJ in the thumb (residues 286–290). The quality of the electron-density map is poor in these regions, but two contacts can be assigned: a bond between Arg-78 and the main chain of the thumb, and a nonpolar interaction involving Phe-61 and Leu-289. The total contact area between the domains is small (420 Å^2), and the interaction is probably weak.

Polymerase Active Site. A representation of the polymerase catalytic region is shown in Fig. 4, with side-chain positions indicated for a number of the residues. The β-turn formed from the conserved Tyr-Met-Asp-Asp sequence (residues 183–186) adopts a typical type II′ conformation. This geometry is common in β-hairpins (16), but glycine is strongly preferred as the second residue of the turn. In RT, the methionine at the second position has an unfavorable steric interaction between its Cβ atom and the amide group of Asp-185. A hydrogen bond from the Nε of Gln-182 to the carbonyl oxygen of Met-184 stabilizes this otherwise strained conformation. Formation of the bond requires that the carbonyl oxygen be shifted toward the open end of the hairpin, promoting a type II′ geometry over type I, which would normally be favored. The type II′ conformation of this turn may be needed to precisely position the aspartate residues for catalysis. In retroviral reverse transcriptases, glutamine is the most common residue at positions equivalent to residue 182 (17), and histidine, which could make a similar contact, is second in frequency. Glutamine is also sometimes found at this position in other polymerases, such as bacterial DNA polymerase I (18). Glycine is a common residue at the equivalent of residue 184 (second position of the turn) in many RNA-dependent RNA polymerases and some DNA-dependent DNA polymerases, suggesting that these may have more conventional type II′ turns.

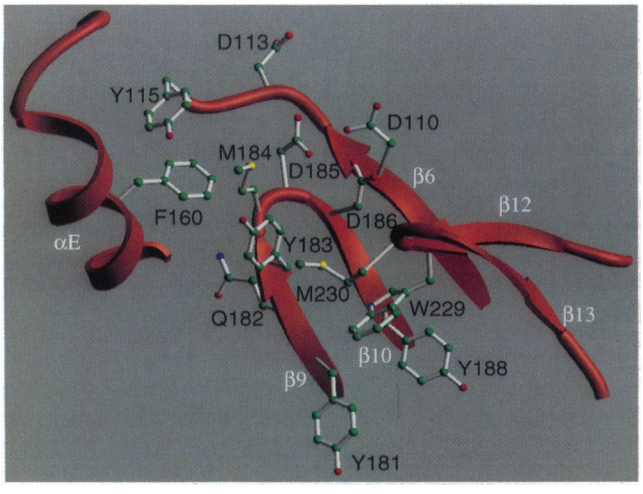

FIG. 4. Polymerase active-site region. Secondary structure elements that form a portion of the polymerase active site are shown, along with side-chain atoms from many of the residues.

An interesting feature of the active-site region is the presence of a cavity that begins immediately adjacent to the β-turn described above and extends down along the p66 fingers domain side of the β9–10 hairpin. Other sides are bounded by residues in αE and β6. The cavity is largely hydrophobic, with side chains from residues Val-111, Phe-160, Met-164, Leu-168, Leu-187, Leu-209, Leu-214, and Leu-241 surrounding the space. Gln-182 and main-chain groups, particularly from β9–10 are also present. The volume of the site is small, but relatively minor side-chain movements might open up more space further toward the base of the β9–10 hairpin. Its proximity to the catalytic residues suggests that this cavity might be considered in attempts to develop novel RT inhibitors.

We thank E. Arnold, T. Steitz, and S. Smerdon for providing coordinates before general release; Martin Rosenberg for continuous support; S. Abdel-Meguid for advice and encouragement; the Biological Process Sciences Department of SmithKline Beecham for preparing cells, and the members of the staff at Cornell High Energy Synchrotron Source (CHESS) and MacChess for help with the x-ray data collection. This work was supported by National Institutes of Health Grants GM39589 (to S.C.H.) and GM39526 (to C.D.), a grant from the American Foundation for AIDS Research, and an American Cancer Society Fellowship (to D.W.R.). S.C.H., S.J.G., and S.R. are with the Howard Hughes Medical Institute.

1. Kohlstaedt, L. A., Wang, J., Friedman, J. M., Rice, P. A. & Steitz, T. A. (1992) *Science* **256,** 1783–1790.
2. Smerdon, S. J., Jäger, J., Wang, J., Kohlstaedt, L. A., Chirino, A. J., Friedman, J. M., Rice, P. A. & Steitz, T. (1994) *Proc. Natl. Acad. Sci. USA* **91,** 3911–3915.
3. Jacobo-Molina, A., Ding, J., Nanni, R., Clark, A. D., Lu, X., Tantillo, C., Williams, R. L., Kamer, G., Ferris, A. L., Clark, P., Hizi, A., Hughes, S. H. & Arnold, E. (1993) *Proc. Natl. Acad. Sci. USA* **90,** 6320–6324.
4. Mizrahi, V., Lazarus, G. M., Miles, L. M., Meyers, C. A. & Debouck, C. (1989) *Arch. Biochem. Biophys.* **273,** 347–358.
5. Taylor, P. B., Culp, J. S., Debouck, C., Johnson, R. K., Patil, A. D., Woolf, D. J., Brooks, I. & Hertzberg, R. P. (1994) *J. Biol. Chem.* **269,** 6325–6331.
6. Teng, T.-Y. (1990) *J. Appl. Crystallogr.* **23,** 387–391.
7. Jones, T. A., Zou, J. Y., Cowan, S. W. & Kjeldgaard, M. (1991) *Acta Crystallogr. A* **47,** 110–119.
8. Navaza, J. (1994) *Acta Crystallogr. A* **50,** 157–163.
9. Kleywegt, G. J. & Jones, T. A. (1994) in *From First Map to Final Model*, eds. Bailey, S., Hubbard, R. & Waller, D. (Science and Engineering Research Council, Daresbury Laboratory, Daresbury, U.K.), pp. 59–66.
10. Brünger, A. T. (1992) XPLOR program manual (Yale Univ., New Haven, CT), Version 3.1.
11. Carson, M. (1987) *J. Mol. Graphics* **5,** 103–106.
12. Nanni, R. G., Ding, J., Jacobo-Molina, A., Hughes, S. H. & Arnold, A. (1993) *Prospect. Drug Discovery Des.* **1,** 129–150.
13. Debyser, Z., Pauwels, R., Andries, K., Desmyter, J., Kukla, M., Janssen, P. A. J. & De Clercq, E. (1991) *Proc. Natl. Acad. Sci. USA* **88,** 1451–1455.
14. Tramontano, E. & Cheng, Y. (1992) *Biochem. Pharmacol.* **43,** 1371–1376.
15. Bacolla, A., Shih, C.-K., Rose, J. M., Piras, G., Warren, T. C., Grygon, C. A., Ingraham, R. H., Cousins, R. C., Greenwood, D. J., Richman, D., Cheng, Y.-C. & Griffin, J. A. (1993) *J. Biol. Chem.* **268,** 16571–16577.
16. Sibanda, B. L., Blundell, T. L. & Thornton, J. M. (1989) *J. Mol. Biol.* **206,** 759–777.
17. Poch, O., Sauvaget, I., Delarue, M. & Tordo, N. (1989) *EMBO J.* **8,** 3867–3874.
18. Delarue, M., Olivier, P., Tordo, N., Moras, D. & Argos, P. (1990) *Protein Eng.* **3,** 461–467.